Advances in Concrete Construction, *Vol. 7, No. 1 (2019) 51-63*
DOI: https://doi.org/10.12989/acc.2019.7.1.051

Dynamic analysis of concrete column reinforced with Sio_2 nanoparticles subjected to blast load

Masoud Azmi, Reza Kolahchi* and Mahmood Rabani Bidgoli

Department of Civil Engineering, Jasb Branch, Islamic Azad University, Jasb, Iran

(Received July 20, 2018, Revised January 14, 2019, Accepted January 15, 2019)

Abstract. The project focuses on the dynamic analysis of concrete beams reinforced with silica-nanoparticles under blast loading. The structure is located at two boundary conditions. The equivalent composite properties are determined using Mori-Tanak model. The structure is simulated with sinusoidal shear deformation theory. Employing nonlinear strains-displacements, stress-strain, the energy equations of beam were obtained and using Hamilton's principal, the governing equations were derived. Using differential quadrature methods (DQM) and Newmark method, the dynamic deflection of the structure is obtained. The influences of volume percent and agglomeration of silica nanoparticles, geometrical parameters of beam, boundary condition and blast load on the dynamic deflection were investigated. Results showed that with increasing volume percent of silica nanoparticles, the dynamic deflection decreases.

Keywords: dynamic analysis; concrete beam; DQM; silica nanoparticle

1. Introduction

Today, there are many applications of continuous mechanics models for structural modeling. A comparison of the results of the atomic modeling and continuum environment mechanics shows that there is an acceptable result continuous mechanical modeling in the estimation of the dynamic behavior of systems. Therefore, most researchers use continuous mechanical modeling to study the dynamic and static behavior of different structures. In recent years, theoretical and laboratory studies are performed on nano-composites. There are applications of this structure in industries, because it's possible to improve the static and dynamic behavior of structures using excellent mechanical and thermal properties of nanoparticles as a booster. Mesia and Seldato (1999) studied as free vibrations of composite-cylindrical shells. To calculate the equivalent properties of the composite, Tan and Wang (2001) presented the micro-electromechanical model. The study of free vibrations of composite-cylindrical shells containing fluid flow is performed by Cadoli and Jensen (2003). Dynamic behavior of composite cylindrical shell containing fluid flow was investigated by Seo and his colleagues (2015). White and Adali (2005) performed a carbon nanotube reinforced beams stress analysis. They concluded that the presence of carbon nanotubes as a booster phase could increase the stability and toughness of the system. Also, Matsuna (2007) investigated the stability of a composite-cylindrical shell using a third-order shear theory. Formaica (2010) examined the vibrations of reinforced sheets of carbon-nanotubes and used the Muritha-Tanaka model to equate the properties of a composite equivalent. Liu and his colleagues (2014) studied the buckling analysis of nano-composite shells. In this study, the mixing rule was used to obtain the equivalent properties of the nano-composite and also selected the Non-mesh method for analyzing the buckling load of the nano-composite structure. In another similar work, Lee and colleagues (2014) analyzed the dynamic stability of carbon-nanotube reinforced panels. They used the Ashley Bai-Murita Tanaka model to equate the properties of nano-composites and with the help of Ritz's method, obtained the range of system instability. The stress of cylindrical shells reinforced with carbon a nanotube was analyzed by GhorbanpurArani *et al*. (2015) which was placed under anomalous heat load, uniform electrical and magnetic charge. Finally, the stresses were calculated using DQM method. Buckling of Carbon-Nanotubes Reinforced Polymer plates was conducted by Kolahchi *et al*. (2013), which was used in the mixing rule to compute the equivalent properties of a composite in this research, and used DQM method to obtain the buckling load of the structure. In another study, the dynamical buckling of reinforced plates with formulated carbon nanotubes was evaluated in functional form by Kolahchi *et al*. (2016). The properties of the plate were temperature dependent and simulated the elastic environment surrounding the structure with the orthotropic Pasternak model. There are very limited researches, in the field of mathematical modeling of concrete structures. As an example, we can point to the work of the by Kolahchi *et al*. (2016), where simulated buckling of concrete beams was reinforced with carbon-nanotubes using Euler-Bernoulli and Timoshenko beam models. Large amplitude vibration problem of laminated composite spherical shell panel under combined temperature and moisture environment was analyzed by

*Corresponding author, Ph.D.
E-mail: r.kolahchi@gmail.com

ISSN: 2287-5301 (Print), 2287-531X (Online)

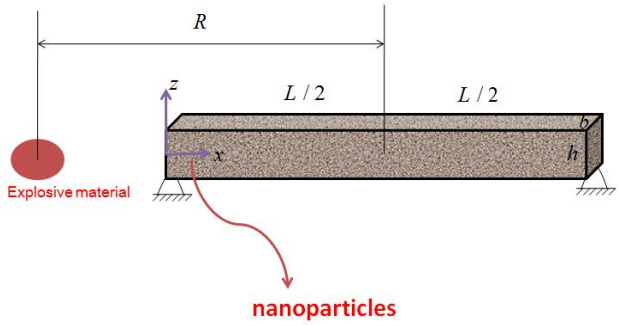

Fig. 1 Concrete beam reinforced with silica-nanoparticles under blast load

Mahapatra *et al*. (2016a). The nonlinear free vibration behaviour of laminated composite spherical shell panel under the elevated hygrothermal environment was investigated by Mahapatra and Panda (2016b). Mahapatra *et al*. (2016c) studied the geometrically nonlinear transverse bending behavior of the shear deformable laminated composite spherical shell panel under hygro-thermo-mechanical loading. Nonlinear free vibration behavior of laminated composite curved panel under hygrothermal environment was investigated by Mahapatra *et al*. (2016d). Nonlinear flexural behaviour of laminated composite doubly curved shell panel was investigated by Mahapatra *et al*. (2016e) under hygro-thermo-mechanical loading by considering the degraded composite material properties through a micromechanical model. Examined Arbabi *et al*. (2017) buckling columns were reinforced with silica nanoparticles under an electric field. The effect of an accumulation on the buckling behavior of concrete columns reinforced with nanoparticles of oxide-silica was investigated by Zamaniyan *et al*. (2017). The flexural behaviour of the laminated composite plate embedded with two different smart materials (piezoelectric and magnetostrictive) and subsequent deflection suppression were investigated by Dutta *et al*. (2017). Suman *et al*. (2017) studied static bending and strength behaviour of the laminated composite plate embedded with magnetostrictive (MS) material numerically using commercial finite element tool. Also, it was devoted to the seismic analysis of concrete pipes reinforced with silica nano-particles using numerical methods by Motazaker *et al*. (2017). Shim *et al*. (2018) studied Crack control of precast deck loop joint cusing high strength concrete. Alhatmey *et al*. (2018) presented residual strength capacity of fire exposed circular concrete-filled steel tube stub columns.

According to the search in the world scientific databases, no work has been done on the mathematical modeling of concrete columns under the blast load. This issue is of great importance in the field of engineering and nano-composites. Therefore, the project focuses on the dynamic analysis of concrete beams reinforced with silica-nanoparticles under blast loading. For this purpose, reinforced concrete beams used silica nano-particles and equilibrated concrete properties through the Mori-Tanaka model. The equivalence equation is based on the volumetric percentage of nanoparticles that can be studied by changing the effect of nanotechnology on stability. Also, the structure is modeled using the theory of sinusoidal shear beam mathematically and the DQM method is used to obtain the dynamic gradient of the structure.

2. Mathematical modeling

Fig. 1 shows a reinforced beams of silica Nano sizedparticles of length *L*. This ball is located on two supports. A blast hole is located at a distance R from the center of the concrete beam.

3. Sinusoil shear deformation theory

There are many new theories for modeling of different structures. Some of the new theories have been used by Tounsi and co-authors (Bessaim 2013, Bouderba 2013, Belabed 2014, Ait Amar Meziane 2014, Zidi 2014, Hamidi 2015, Bourada 2015, Bousahla *et al*. 2016a, b, Beldjelili 2016, Boukhari 2016, Draiche 2016, Bellifa 2015, Attia 2015, Mahi 2015, Ait Yahia 2015, Bennoun 2016, El-Haina 2017, Menasria 2017, Chikh 2017, Zemri 2015, Larbi Chaht 2015, Belkorissat 2015, Ahouel 2016, Bounouara 2016, Bouafia 2017, Besseghier 2017, Bellifa 2017, Mouffoki 2017, Khetir 2017).

The assumptions of this theory are:

1. There are small displacements in comparison with the thickness of the page and consequently, the strains are small.

2. The normal transverse tensile (σ_{zz}) is irrelevant compared to the stresses of the plate σ_{xx} and σ_{yy}.

3. The transverse displacement (w) consists of two bandings (w_b) and (w_s) shear sections, which are functions of the frets x and y time t.

So:

$$w(x,y,z,t) = w_b(x,y,t) + w_s(x,y,t) \tag{1}$$

4. The in-leaf displacements u and v are made up of three sections: tensile, bending and shear.

So

$$u(x,y,z,t) = u(x,y,t) + u_b(x,y,t) + u_s(x,y,t) \tag{2}$$

$$v(x,y,z,t) = v(x,y,t) + v_b(x,y,t) + v_s(x,y,t) \tag{3}$$

Where

$$u_b = -z\frac{\partial w_b}{\partial x} \tag{4}$$

$$v_b = -z\frac{\partial w_b}{\partial y} \tag{5}$$

Shear components u_s, v_s and w_s expresses the sinusoidal changes of shear strains γ_{xz} and γ_{yz}. Therefore, u_s and v_s are written according to w_s as the followings

$$u_s = -\left(z - \frac{h}{\pi}\sin\frac{\pi z}{h}\right)\frac{\partial w_s}{\partial x} \tag{6}$$

$$v_s = -\left(z - \frac{h}{\pi} \sin \frac{\pi z}{h} \right) \frac{\partial w_s}{\partial y} \tag{7}$$

According to the assumptions given, the displacement field of this theory for the beam is as follows

$$u_1(x,z,t) = u(x,t) - z\frac{\partial w(x,t)}{\partial x} + f\psi(x,t)\,, \tag{8}$$

$$u_3(x,z,t) = w(x,t)\,, \tag{9}$$

$$u_2(x,z,t) = 0\,, \tag{10}$$

While u_1, u_2 and u_3 are the displacement of the points of the center plan in the longitudinal, transverse and thick direction. Also, $f = \frac{h}{\pi}\sin\left(\frac{\pi z}{h}\right)$ and ψ is rotation of cross-section around the y axis.

The stress-strain non-linear displacement of the structure is based on the theory of von-carmen as follows.

By placing the relationships (8) to (10) in the above relations, the Von-karmen type nonlinear strain-displacement relations are given by

$$\varepsilon_{xx} = \frac{\partial u}{\partial x} - z\frac{\partial^2 w}{\partial x^2} + \frac{1}{2}\left(\frac{\partial w}{\partial x}\right)^2 + f\frac{\partial \psi}{\partial x}, \tag{11}$$

$$\varepsilon_{xz} = \cos\left(\frac{\pi z}{h}\right)\psi, \tag{12}$$

4. Stress-strain equations

According to Hooke's law

$$\begin{bmatrix} \sigma_{xx} \\ \sigma_{yy} \\ \sigma_{zz} \\ \tau_{yz} \\ \tau_{xz} \\ \tau_{xy} \end{bmatrix} = \begin{bmatrix} Q_{11} & Q_{12} & Q_{13} & 0 & 0 & 0 \\ Q_{12} & Q_{22} & Q_{23} & 0 & 0 & 0 \\ Q_{13} & Q_{23} & Q_{33} & 0 & 0 & 0 \\ 0 & 0 & 0 & Q_{44} & 0 & 0 \\ 0 & 0 & 0 & 0 & Q_{55} & 0 \\ 0 & 0 & 0 & 0 & 0 & Q_{66} \end{bmatrix} \begin{Bmatrix} \varepsilon_{xx} \\ \varepsilon_{yy} \\ \varepsilon_{zz} \\ \gamma_{yz} \\ \gamma_{xz} \\ \gamma_{xy} \end{Bmatrix}, \tag{13}$$

Q_{ij}'s are elastic constants. According to the sinusoidal shear deformation theory

$$\sigma_{xx} = Q_{11}\varepsilon_{xx}\,, \tag{14}$$

$$\sigma_{xz} = Q_{55}\varepsilon_{xz}\,, \tag{15}$$

5. Energy method and the Hamilton law

The potential energy of the structure is written as follows

$$U = \frac{1}{2}\int_V \left(\sigma_{xx}\varepsilon_{xx} + \sigma_{xz}\varepsilon_{xz}\right) dV\,, \tag{16}$$

Submitting Eqs. (11) and (12) into (16), the potential energy give as follows

$$U = \frac{1}{2}\int_V \left(\sigma_{xx}\left(\frac{\partial u}{\partial x} - z\frac{\partial^2 w}{\partial x^2} + \frac{1}{2}\left(\frac{\partial w}{\partial x}\right)^2 + f\frac{\partial \psi}{\partial x} \right) + \sigma_{xz}\left(\cos\left(\frac{\pi z}{h}\right)\psi \right) \right) dV\,, \tag{17}$$

The forces and moment within the page are defined as follows

$$\left(N_x, M_x, P_x\right) = \int_A \left(1, z, f\right)\sigma_x dA, \tag{18}$$

$$Q_x = \int_A \cos\left(\frac{\pi z}{h}\right)\sigma_{xz} dA, \tag{19}$$

Simplifies the potential energy as follows

$$U = \int_x \left(N_x\frac{\partial u}{\partial x} + \frac{N_x}{2}\left(\frac{\partial w}{\partial x}\right)^2 - M_x\frac{\partial^2 w}{\partial x^2} + P_x\frac{\partial \psi}{\partial x} + Q_x\psi \right) dx \tag{20}$$

The kinetic energy of concrete beam is calculated as follows

$$K = \frac{1}{2}\rho\int_A\int_{-\frac{h}{2}}^{\frac{h}{2}} \left(\left(\frac{\partial u_1}{\partial t}\right)^2 + \left(\frac{\partial u_2}{\partial t}\right)^2 + \left(\frac{\partial u_3}{\partial t}\right)^2 \right) \mathrm{dz\,dA}. \tag{21}$$

Submitting Eqs. (8) and (10) into above equations as follows

$$K = 0.5\int \left(I_0\left(\left(\frac{\partial u}{\partial t}\right)^2 + \left(\frac{\partial w}{\partial t}\right)^2 \right) - I_1\frac{\partial u}{\partial t}\frac{\partial w}{\partial t\partial x} + I_2\left(\frac{\partial w}{\partial t\partial w}\right)^2 + I_3\left(\frac{\partial \psi}{\partial t}\right)^2 + 2I_4\frac{\partial w}{\partial t\partial x}\frac{\partial \psi}{\partial t} + 2I_5\frac{\partial u}{\partial t}\frac{\partial \psi}{\partial t} \right) dA. \tag{22}$$

Moment of inertia of mass is

$$\left(I_0, I_1, I_2, \mathrm{I}_3, I_4, I_5\right) = \int_{-h}^{h} \rho\left(1, z, z^2, f^2, zf, f\right). \tag{23}$$

External work caused by the blast force is

$$W_b = \int \left(F_{blast}\right) w dA, \tag{24}$$

Where

$$P_{blast} = P_{S0}\left[1 - \frac{t}{t_0}\right]\exp\left\{\frac{-at}{t_0}\right\}, \tag{25}$$

Where P_{S0} is the maximum static pressure and t_0 is positive phase time. That they are

$$\frac{P_{S0}}{P_0} = \frac{808\left[1 + \left(\frac{Z}{4.5}\right)^2\right]}{1 + \left(\frac{Z}{0.048}\right)^2\sqrt{1 + \left(\frac{Z}{1.35}\right)^2}}, \tag{26}$$

$$\frac{t_0}{W^{1/3}}=\frac{980\left[1+\left(\frac{Z}{0.54}\right)^{10}\right]}{\left[1+\left(\frac{Z}{0.02}\right)^{3}\right]\left[1+\left(\frac{Z}{0.74}\right)^{6}\right]\sqrt{1+\left(\frac{Z}{6.9}\right)^{2}}}, \quad (27)$$

Where P_0 is the air pressure.

$$Z=\frac{R}{W^{0.33}}, \quad (28)$$

In the above relation, R is distance from blast center to surface of structure and W is the explosive mass in terms of Kg.

Expressed as Hamilton's principle

$$\int_0^t(\delta U-\delta K-\delta W_b)dt=0, \quad (29)$$

In the above relations, δ is system energy changes. The following three equations obtained by submitting Eqs. (20), (22) and (24) into Eq. (29) and using partial integration and ordering relations in the direction of mechanical displacements:

Eq. (1): by separating δu factors

$$\delta u:\frac{\partial N_x}{\partial x}=I_0\frac{\partial^2 u}{\partial t^2}-\mathrm{I}_1\frac{\partial^3 w}{\partial t^2\partial x}+\mathrm{I}_5\frac{\partial^2\psi}{\partial t^2}, \quad (30)$$

Eq. (2): by separating δw factors

$$\delta w:\frac{\partial^2 M_x}{\partial x^2}+2\mathrm{e}_{31}\mathrm{V}_0\frac{\partial^2 w}{\partial x^2}+P_{blast}=I_0\frac{\partial^2 w}{\partial t^2}+\mathrm{I}_1\frac{\partial^3 u}{\partial t^2\partial x}-\mathrm{I}_2\frac{\partial^4 w}{\partial t^2\partial x^2}+\mathrm{I}_5\frac{\partial^3\psi}{\partial t^2\partial x}, \quad (31)$$

Eq. (3): by separating $\delta\psi$ factors

$$\delta\psi:\frac{\partial P_x}{\partial x}-Q_x=I_3\frac{\partial^2\psi}{\partial t^2}-I_4\frac{\partial^3 w}{\partial t^2\partial x}+I_5\frac{\partial^2 u}{\partial t^2}, \quad (32)$$

Can be calculated relations of forces and internal moments of beam, by submitting Eqs. (14) and (15) into Eqs. (18) and (19)

$$N_x=hQ_{11}\frac{\partial u}{\partial x}+\frac{hQ_{11}}{2}\left(\frac{\partial w}{\partial x}\right)^2, \quad (33)$$

$$M_x=-Q_{11}I\frac{\partial^2 w}{\partial x^2}+\frac{24Q_{11}I}{\pi^3}\frac{\partial\psi}{\partial x}, \quad (34)$$

$$P_x=-\frac{24Q_{11}I}{\pi^3}\frac{\partial^2 w}{\partial x^2}+\frac{6Q_{11}I}{\pi^2}\frac{\partial\psi}{\partial x}, \quad (35)$$

$$Q_x=\frac{Q_{55}A}{2}\psi, \quad (36)$$

Where

$$(A,I)=\int_A\left(1,z^2\right)dA, \quad (37)$$

Now, by submitting Eqs. (33) to (36) into Eqs. (30) to (32), we obtained relations formed in terms of mechanical displacements. These relations are

$$\delta u:\frac{\partial^2 u}{\partial x^2}+\frac{\partial w}{\partial x}\frac{\partial^2 w}{\partial x^2}=I_0\frac{\partial^2 u}{\partial t^2}-\mathrm{I}_1\frac{\partial^3 w}{\partial t^2\partial x}+\mathrm{I}_5\frac{\partial^2\psi}{\partial t^2}, \quad (38)$$

$$\delta w:-Q_{11}I\frac{\partial^4 w}{\partial x^4}+\frac{24Q_{11}I}{\pi^3}\frac{\partial^3\psi}{\partial x^3}+P_{blast}=I_0\frac{\partial^2 w}{\partial t^2}+\mathrm{I}_1\frac{\partial^3 u}{\partial t^2\partial x}-\mathrm{I}_2\frac{\partial^4 w}{\partial t^2\partial x^2}+\mathrm{I}_5\frac{\partial^3\psi}{\partial t^2\partial x}, \quad (39)$$

$$\delta\psi:-\frac{24Q_{11}I}{\pi^3}\frac{\partial^3 w}{\partial x^3}+\frac{6Q_{11}I}{\pi^2}\frac{\partial^2\psi}{\partial x^2}-\frac{Q_{55}A}{2}\psi=I_3\frac{\partial^2\psi}{\partial t^2}-I_4\frac{\partial^3 w}{\partial t^2\partial x}+I_5\frac{\partial^2 u}{\partial t^2}, \quad (40)$$

The associated boundary conditions can be expressed:

• Clamped- Clamped boundary condition(C-C)

$$\begin{aligned} &w=u=\varphi=\psi=0, && @\quad x=0\\ &w=u=\varphi=\psi=0. && @\quad x=L\end{aligned} \quad (41)$$

• Clamped -simply boundary condition(C-S)

$$\begin{aligned} &w=u=\phi=\psi=0, && @\quad x=0\\ &w=u=\phi=\frac{\partial\psi}{\partial x}=0. && @\quad x=L\end{aligned} \quad (42)$$

• Simply -simply boundary condition(S-S)

$$\begin{aligned} &w=u=\phi=\frac{\partial\psi}{\partial x}=0, && @\quad x=0\\ &w=u=\phi=\frac{\partial\psi}{\partial x}=0. && @\quad x=L\end{aligned} \quad (43)$$

6. Mori-Tanaka model

The properties and elastomeric factors of beam reinforced with silica nanoparticles from a micro-mechanical perspective. Assumed the concrete beam is isotropic beam, Yank Module and poison's ratio are respectively E_m and ν_m. It's assumed that silica nano-particles have transverse elastic properties and consequently, the desired structure has transverse elastic properties. In this case, the stress-strain of relation is expressed in the local coordinates of an elemental element as follows

$$\begin{Bmatrix}\sigma_{11}\\ \sigma_{22}\\ \sigma_{33}\\ \sigma_{23}\\ \sigma_{13}\\ \sigma_{12}\end{Bmatrix}=\begin{bmatrix}k+m & l & k-m & 0 & 0 & 0\\ l & n & l & 0 & 0 & 0\\ k-m & l & k+m & 0 & 0 & 0\\ 0 & 0 & 0 & p & 0 & 0\\ 0 & 0 & 0 & 0 & m & 0\\ 0 & 0 & 0 & 0 & 0 & p\end{bmatrix}\begin{Bmatrix}\varepsilon_{11}\\ \varepsilon_{22}\\ \varepsilon_{33}\\ \gamma_{23}\\ \gamma_{13}\\ \gamma_{12}\end{Bmatrix} \quad (44)$$

In the above relation k, l, m, n, p are Hil elastic modulus, in which k is volumetric modulus of elasticity that it's Perpendicular to direction of the fiber. n is tensile modulus abaxial in the longitudinal direction of the fibers, l is Cross-sectional modulus, m and p are respectively, shear modulus in the parallel and vertical sides of fibers. The Hil elastic modulus is obtained by using Murray-Tanaka method as follows

$$k=\frac{E_m\{E_m c_m+2k_r(1+\nu_m)[1+c_r(1-2\nu_m)]\}}{2(1+\nu_m)[E_m(1+c_r-2\nu_m)+2c_m k_r(1-\nu_m-2\nu_m^2)]}$$

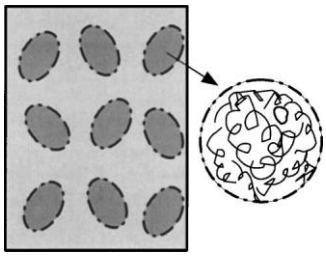

Fig. 2 Selected volumetric element of nano-composite

$$l=\frac{E_m\{c_m\nu_m[E_m+2k_r(1+\nu_m)]+2c_rl_r(1-\nu_m^2)]\}}{(1+\nu_m)[E_m(1+c_r-2\nu_m)+2c_mk_r(1-\nu_m-2\nu_m^2)]}$$

$$n=\frac{E_m^2c_m(1+c_r-c_m\nu_m)+2c_mc_r(k_rn_r-l_r^2)(1+\nu_m)^2(1-2\nu_m)}{(1+\nu_m)[E_m(1+c_r-2\nu_m)+2c_mk_r(1-\nu_m-2\nu_m^2)]}$$
$$+\frac{E_m[2c_m^2k_r(1-\nu_m)+c_rn_r(1+c_r-2\nu_m)-4c_ml_r\nu_m]}{E_m(1+c_r-2\nu_m)+2c_mk_r(1-\nu_m-2\nu_m^2)}$$

$$p=\frac{E_m[E_mc_m+2p_r(1+\nu_m)(1+c_r)]}{2(1+\nu_m)[E_m(1+c_r)+2c_mp_r(1+\nu_m)]}$$

$$m=\frac{E_m[E_mc_m+2m_r(1+\nu_m)(3+c_r-4\nu_m)]}{2(1+\nu_m)\{E_m[c_m+4c_r(1-\nu_m)]+2c_mm_r(3-\nu_m-4\nu_m^2)\}} \tag{45}$$

In the above relations, k_r, l_r, n_r, p_r, mrare the Hil elastic modulus for reinforced phase (silica- nanoparticles). Finally, the hardness matrix is obtained by calculating parameters*k*, *l*, *m*, *n*, *p*. Experimental results show that more nano-particles are irregular in concrete. It's observed that a large part of the nano-particles are concentrated inside the concrete in a region.It's assumed this region is spherical and is the so-called, capacity, Which is different from its properties with the material around it. A volumetric element of it is shown, in the Fig. 2.

V_r is the final volume of the nanoparticles where

$$V_r=V_r^{inclusion}+V_r^m \tag{46}$$

Which respectively $V_r^{inclusion}$, V_r^m are the volumes of nano-particles in the capacity and concrete.The two parameters below are used to show accumulation effect in the micro-mechanical model

$$\xi=\frac{V_{inclusion}}{V}, \tag{47}$$

$$\zeta=\frac{V_r^{inclusion}}{V_r}. \tag{48}$$

The average volume fraction of nanoparticles in a concrete beam C_r is given as follows

$$C_r=\frac{V_r}{V}. \tag{49}$$

The relation of volume fraction nano-particles to capacity and concrete using the above relations is as follows

$$\frac{V_r^{inclusion}}{V_{inclusion}}=\frac{C_r\zeta}{\xi}, \tag{50}$$

$$\frac{V_r^m}{V-V_{inclusion}}=\frac{C_r(1-\zeta)}{1-\xi}. \tag{51}$$

Assuming nanoparticles are the transverse isotropic and located completely random in the capacity, and also assuming Capacity Isotropic, volumetric modulus *k* and the shear modulus *G* sing Mori-Tanaka method for isotropic materials are defined as follows

$$K=K_{out}\left[1+\frac{\xi\left(\frac{K_{in}}{K_{out}}-1\right)}{1+\alpha(1-\xi)\left(\frac{K_{in}}{K_{out}}-1\right)}\right], \tag{52}$$

$$G=G_{out}\left[1+\frac{\xi\left(\frac{G_{in}}{G_{out}}-1\right)}{1+\beta(1-\xi)\left(\frac{G_{in}}{G_{out}}-1\right)}\right], \tag{53}$$

In the above relations K_{in} and K_{out} are respectively, volumetric modulus capacity and composite minus the capacity and also omitted, Ginand Goutshear modulus capacity and composite minus the capacities which were obtained from the following relations

$$K_{in}=K_m+\frac{(\delta_r-3K_m\chi_r)C_r\zeta}{3(\xi-C_r\zeta+C_r\zeta\chi_r)}, \tag{54}$$

$$K_{out}=K_m+\frac{C_r(\delta_r-3K_m\chi_r)(1-\zeta)}{3[1-\xi-C_r(1-\zeta)+C_r\chi_r(1-\zeta)]}, \tag{55}$$

$$G_{in}=G_m+\frac{(\eta_r-3G_m\beta_r)C_r\zeta}{2(\xi-C_r\zeta+C_r\zeta\beta_r)}, \tag{56}$$

$$G_{out}=G_m+\frac{C_r(\eta_r-3G_m\beta_r)(1-\zeta)}{2[1-\xi-C_r(1-\zeta)+C_r\beta_r(1-\zeta)]}, \tag{57}$$

Where χ_r, β_r, δ_r, η_r are

$$\chi_r=\frac{3(K_m+G_m)+k_r-l_r}{3(k_r+G_m)}, \tag{58}$$

$$\beta_r=\frac{1}{5}\left\{\frac{4G_m+2k_r+l_r}{3(k_r+G_m)}+\frac{4G_m}{(p_r+G_m)}\right.$$
$$\left.+\frac{2[G_m(3K_m+G_m)+G_m(3K_m+7G_m)]}{G_m(3K_m+G_m)+m_r(3K_m+7G_m)}\right\}, \tag{59}$$

$$\delta_r=\frac{1}{3}\left[n_r+2l_r+\frac{(2k_r-l_r)(3K_m+2G_m-l_r)}{k_r+G_m}\right], \tag{60}$$

$$\eta_r=\frac{1}{5}\left[\frac{2}{3}(n_r-l_r)+\frac{4G_mp_r}{(p_r+G_m)}\right.$$
$$\left.+\frac{8G_mm_r(3K_m+4G_m)}{3K_m(m_r+G_m)+G_m(7m_r+G_m)}+\frac{2(k_r-l_r)(2G_m+l_r)}{3(k_r+G_m)}\right]. \tag{61}$$

Also, K_m and G_m are volumetric and shear modulus of the base phase

$$K_m = \frac{E_m}{3(1-2\upsilon_m)} \quad , \tag{62}$$

$$G_m = \frac{E_m}{2(1+\upsilon_m)}. \tag{63}$$

Also, β, α in the equations stated before (52) and (53) are defined by the following relations

$$\alpha = \frac{(1+\upsilon_{out})}{3(1-\upsilon_{out})} \quad , \tag{64}$$

$$\beta = \frac{2(4-5\upsilon_{out})}{15(1-\upsilon_{out})}, \tag{65}$$

$$\upsilon_{out} = \frac{3K_{out} - 2G_{out}}{6K_{out} + 2G_{out}}. \tag{66}$$

Through obtaining volume modulus K and shear modulus G of the nano-composite, E and υ of composite isotropic material will be achieved by using the above relations as following

$$E = \frac{9KG}{3K+G} \quad , \tag{67}$$

$$\upsilon = \frac{3K-2G}{6K+2G}. \tag{68}$$

Finally, stiffness matrix of structure with E and υ is computed.

7. DQM method

Differential quadrature method (DQM) is a numerical method, which converts the governing differential equations into first-order algebraic equations using weighting coefficients. Thus at each point, the derivatives will be expressed as a linear sum of weighting coefficients ,values of the function at that point and other points of domain and in the direction axes of coordinate. The main relation of these methods for one-dimensional state

$$\frac{d^n f(x_i)}{dx^n} = \sum_{j=1}^{N} C_{ij}^{(n)} f(x_j) \qquad n = 1,...,N-1. \tag{69}$$

$f(x)$ is desired function, N isnumber of sample points, x_i is the sample point i of the function amplitude, f_i is value of function at sample point i and C_{ij} is weighting coefficients to obtain derivative of function at the sample point i. Therefore, it can be seen that two most important factors in differential quadrature method are selection of sample points and weighting coefficients.

8. Chebyshev polynomial roots

To obtain sample points, we apply Chebyshev polynomial roots which get good results as the following

$$X_i = \frac{L}{2}\left[1 - \cos\left(\frac{i-1}{N_x - 1}\right)\pi\right] \qquad i = 1,...,N_x \tag{70}$$

9. Weighting coefficients

To apply the square differential method to solve a differential equation, we must write the derivatives as the matrix product of the weight coefficients in the unknown vector. Thus, Bellman introduced the test function using Lagrange's transmitted orthogonal polynomial, according to the following equation

$$g(x) = \frac{L(x)}{(x-x_i)L_1(x_i)} \qquad i = 1,2,...,N \tag{71}$$

$$g(x) = a_{N-1}x^{N-1} + a_{N-2}x^{N-2} + ... + a_1 x + a_0, \tag{a}$$

As N is the number of sample points and $L(x)$ is Lagrange's orthogonal polynomial function of order N.

$$L(x) = \prod_{j=1}^{N}(x - x_j) \qquad i \neq j \tag{72}$$

Where defined, derivative of by Lagrange's transmitted orthogonal polynomial function from order N is as follows

$$L_i(x) = \prod_{j=1}^{N}(x_i - x_j) \tag{73}$$

By selecting Lagrange's orthogonal polynomial roots as sample points and substituting $g(x)$ into Eq. (a), a simple algebraic relations for calculating weighting coefficients is obtained

$$C_{ij}^{(1)} = \frac{L_1(x_i)}{(x_i - x_j)L_1(x_j)} \qquad for \quad i \neq j, \quad i, j = 1,2,...,N \tag{74}$$

$$C_{ii}^{(1)} = -\sum_{j=1, j\neq i} C_{ij}^{1} \quad for \quad i = j, \; i = 1,2,...,N. \tag{75}$$

It's possible to multiply first-order weighting coefficient matrix from order n in itself for to obtain weighting coefficient of higher derivatives. That's mean

$$\left[C^{(n)}\right] = \left[C^{(1)}\right]^n \tag{76}$$

10. Applying DQM

To solve the governing equations, Gridding is a concrete beam in length along by Chebyshev and weighting coefficients for all derivatives are calculated using the relation (74) to (76). Then derivatives will be replaced with matrixes of their weighting coefficients. As the result, it's necessary to separate equations of boundary condition and field from each other because of existence of weight coefficients for coupling with governing equations. The governing equations and boundary conditions in the matrix form are written as follows

$$\left(\left[\underbrace{K_L + K_{NL}}_{K}\right]\begin{Bmatrix}\{d_b\}\\ \{d_d\}\end{Bmatrix} + [M]\begin{Bmatrix}\{\ddot{d}_b\}\\ \{\ddot{d}_d\}\end{Bmatrix}\right) = \begin{Bmatrix}\{0\}\\ F\end{Bmatrix}, \tag{77}$$

In the above relation, there are the linear part of stiffness matrix [K], non-linear part of the stiffness matrix [K_{NL}], mass matrix [M], dynamic amplitude vector for boundary

condition points $\{d_b\}$ and dynamic amplitude vector for field conditions$\{d_d\}$.

11. Newmark method

Newmark numerical method is used to obtain the time response of the structure under blast load in domain time. According to this method, Eq. (22) is written in the following general form

$$K^*(d_{i+1}) = Q_{i+1}, \tag{78}$$

Where subtitle i+1 represents time (t=t_{i+1}) $K^*(d_{i+1})$ is effective stiffness matrix and Q_{i+1} is effective load vector written as follows

$$K^*(d_{i+1}) = K_L + K_{NL}(d_{i+1}) + \alpha_0 M, \tag{79}$$

$$Q^*_{i+1} = F_{i+1} + M\left(\alpha_0 d_i + \alpha_2 \dot{d}_i + \alpha_3 \ddot{d}_i\right), \tag{80}$$

Where

$$\alpha_0 = \frac{1}{\chi \Delta t^2}, \quad \alpha_1 = \frac{\gamma}{\chi \Delta t}, \quad \alpha_2 = \frac{1}{\chi \Delta t},$$
$$\alpha_3 = \frac{1}{2\chi} - 1, \quad \alpha_4 = \frac{\gamma}{\chi} - 1, \tag{81}$$
$$\alpha_5 = \frac{\Delta t}{2}\left(\frac{\gamma}{\chi} - 2\right), \quad , \alpha_6 = \Delta t(1-\gamma), \quad \alpha_7 = \Delta t \gamma,$$

Where γ=0.5 and χ=0.25. Based on repeating method, Eq. (23) is solved at each time amplitude and calculates acceleration and speed modifiedfrom the following relations

$$\ddot{d}_{i+1} = \alpha_0 (d_{i+1} - d_i) - \alpha_2 \dot{d}_i - \alpha_3 \ddot{d}_i, \tag{82}$$

$$\dot{d}_{i+1} = \dot{d}_i + \alpha_6 \ddot{d}_i + \alpha_7 \ddot{d}_{i+1}, \tag{83}$$

Then, for the next time, we apply acceleration and speed modified into relations (27) and (28) and the steps mentioned are repeated.

12. Results and charts introduction

In this article, dynamic displacement of concrete beam is calculated using differential quadrature and Newark method, examines the effect of parameters such as percent by volume and percentage of nanoparticles, geometric parameters, boundary conditions and external voltage on dynamics displacement of structure. For this purpose, a concrete beam is considered as with elastic modulus E_m=30 GPa, poison's ratio v_m=0.2, density ρ_m=2500 Kg/m^3, section is 30-by-30-cm, and length is 3 meters, reinforced with silica nano-particles with E_r=60 GPa, also air pressure P_0=100 *mbar*, blast mas W=5 Kg, thedistance between centroid of the concrete beam and blast R=5 m, positive phase time t_a=10 ms and b=1.06.

Validation of results

Until now, it has not been investigated by any researcher, the dynamic analysis of concrete beam reinforced with silica nanoparticles subjected to blast loading by numerical methods. Therefore, to validate the results, dynamical analysis of a concrete beam subjected blast load by sinusoidal shear deformation theory has been studied, by removing effect of silica nanoparticles (C_r=0). Concrete beam is assumed elastic modulus E_m=30 GPa, poison's ratio v_m=0.2, density ρ_m=2500 Kg/m^3, cross-section A=3 m^2, inertial Moment I=0.5625 m^4 and length L=30 m, also air pressure P_0=100 *mbar*, blast mass W=25.5 Kg, Z=2.5, b=1.06 and positive phase time t_a=10 ms. Fig. 3 show dimensionless dynamic displacement of the structure (W^*=w/L) against dimensionless time ($\tau = L\sqrt{\rho_m / kG_m}$) for concrete beam to blast load. As it matches with the reference results, this shows accuracy of the results achieved.

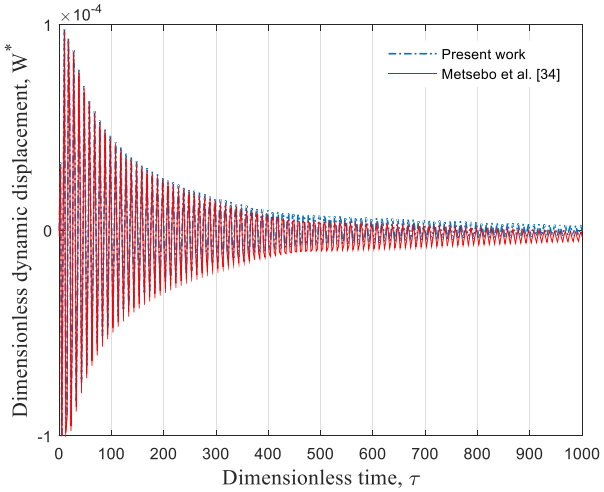

Fig. 3 Comparing the results of this project with reference

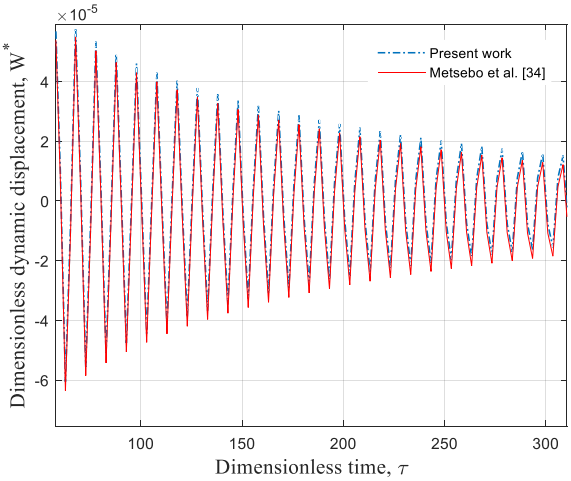

Figure The enlarged view of Fig. 3

13. The effect of different parameters

The effect of percent by volume silica nanoparticles

The effect of percent by volume silica nano-particles on

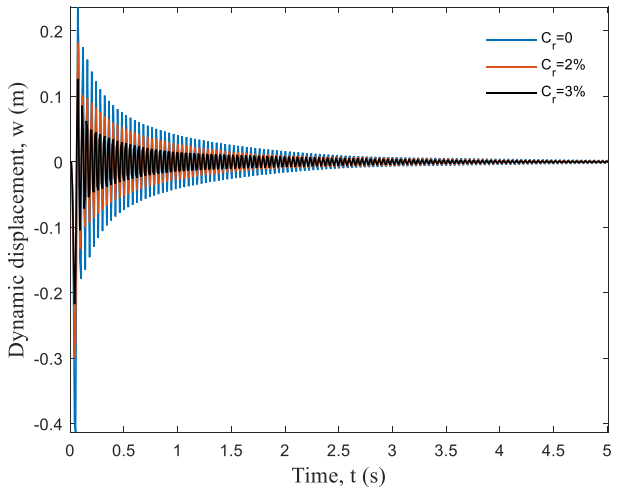

Fig. 4 Effect of percent by volume nanoparticles on dynamic displacement of concrete beam with external voltage applied

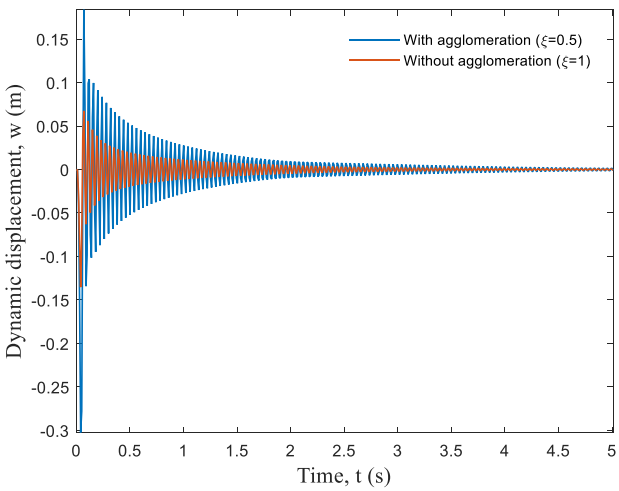

Fig. 6 The effect of nanoparticle accumulation on the dynamic velocity of a concrete beam with the application of external voltage

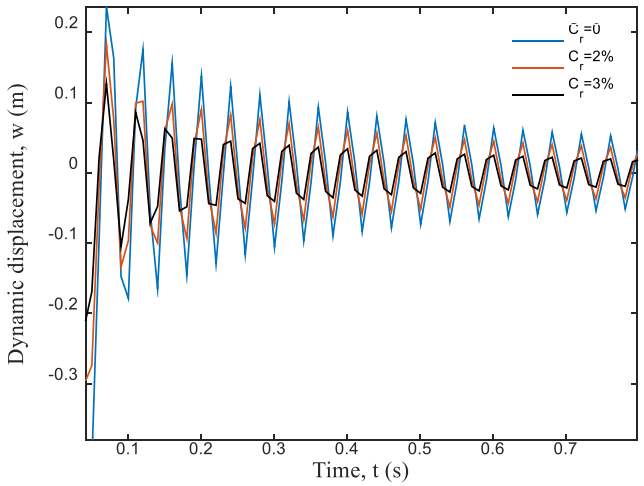

Fig. 5 The enlarged view of Fig. 4

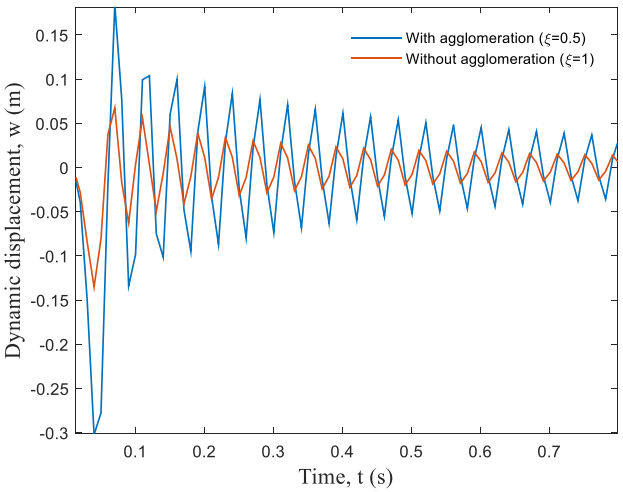

Fig. 7 The enlarged view of Fig. 6

dynamic displacement concrete beam in terms of the blast time is shown in Figs. 4 and 5. Whatever Increase percent by volume of nanoparticles, the decreases the dynamic displacement of the concrete beam.

Maximum dynamicdisplacement for the modes C_r=0 and C_r=2% is respectively 0.23 and 0.19 meters, It decreases by about 20% dynamic displacement with increasing the percent by volume silica nanoparticles. Because of increasing percent by volume silica nanoparticles, there are more nanoparticles in the concrete beam rim. Consequently, it contributes more nanoparticles in the division of load and concrete beams are strengthened due to the high strength of nanoparticles, it increases its strength against the blast load.

As a general result, it can be noted that the use of nanoparticles in reinforcing concrete beams can be effective on the strength of the structure. Of course, it should be noted that it cannot have any amount of percent by volume nanoparticle because it will be reversed from a specific value dynamic behavior of the structure, which requires laboratory testing.

The effect of accumulation of silica nanoparticles

Figs. 6 and 7 show the effect accumulation of silica nanoparticles in a specific area of the concrete beam on dynamic displacement of the structure according to time, as it can be seen, considering the accumulation has reduced the stiffness of the structure and increased dynamic displacement of concrete beam. As a result, there inforcement concrete beam with silica nanoparticles. The less it is, the less will be the accumulation in different places the dynamic displacement structure. For example, the maximum dynamic displacement concrete beam for a state with and without accumulation nano-particles is respectively 0.15 and 0.055 m, this indicates a 67% reduction in the dynamic displacement concrete beam for the distribution of nanoparticles in concrete without accumulation.

The effect of boundary conditions

The effect boundary conditions of two sides concrete

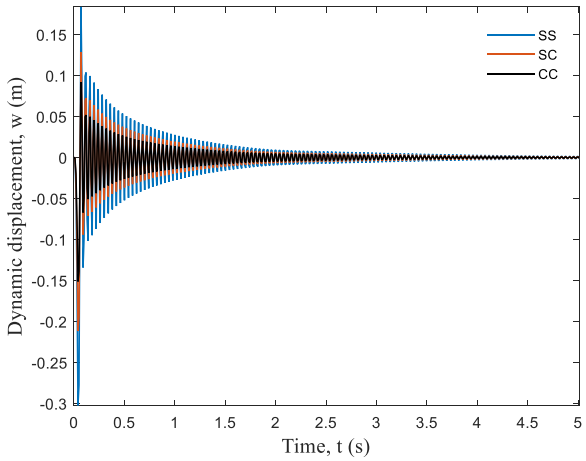

Fig. 8 Effect of boundary conditions on the dynamic gradient of concrete beam with the application of external voltage

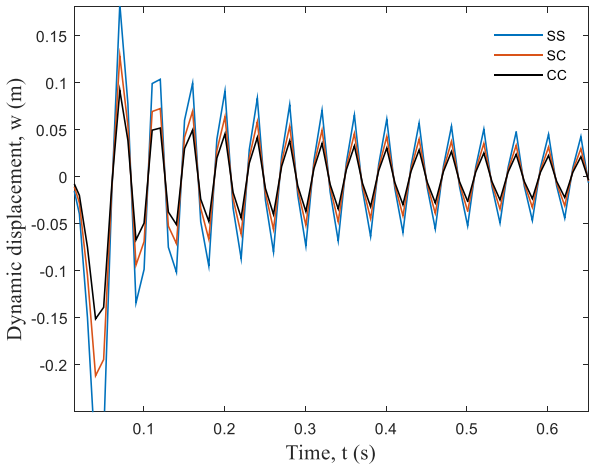

Fig. 9 The enlarged view of Fig. 8

column on dynamic displacement according to the blast are shown in Figs. 8 and 9. There are three boundary conditions clamped- clamped (C-C), clamped- simple (C-S) and simple-simple (S-S). As the boundary conditions are observed, there's a significant effect on structure dynamic displacement, so that concrete beam with fixed and simple boundary conditions, respectively, has a dynamic displacement 0.9 and 0.18 meters at two ends. In other words, a concrete beam with clamping boundary conditions leads to a decrease of about 50% of the maximum dynamic displacement relative to a concrete beam with simple boundary conditions. That's because of the binding structure with a boundary condition at two ends and as the result it's more stiffness. In general, the effect of boundary conditions on dynamic displacement is also respectively a clamped- clamped < clamped- simple < simple-simple.

The effect of vibration mode

Figs. 10 and 11 show the effect of vibration modes in concrete beam on structure dynamic displacement according to time. It's observed that structure dynamic displacement increases with increasing vibrational mode.

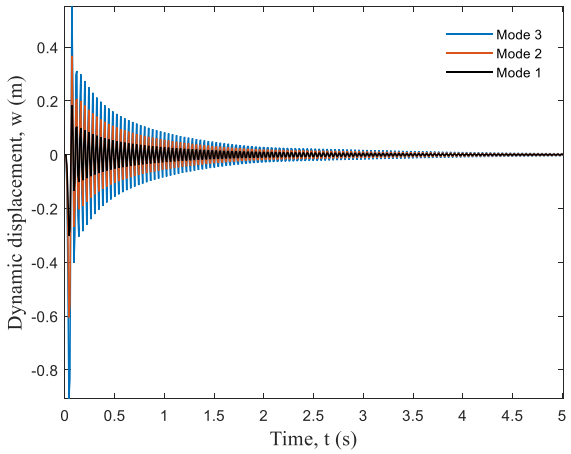

Fig. 10 Effect of damage on concrete beam on dynamic gradient of concrete beam by applying external voltage

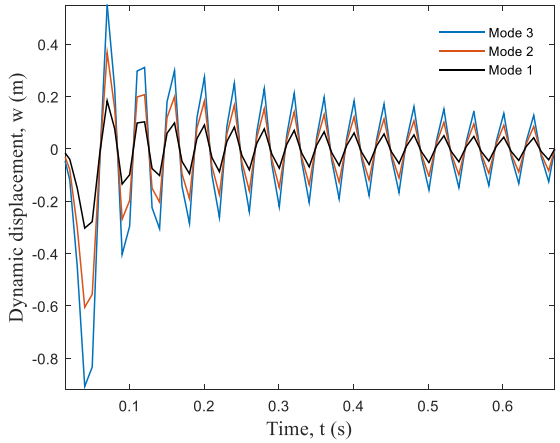

Fig. 11 The enlarged view of Fig. 10

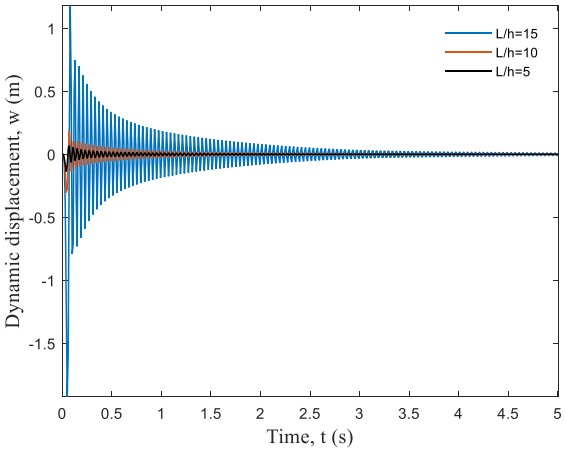

Fig. 12 The effect of the ratio of length to concrete beam thickness on the dynamic gradient of concrete beam with the application of external voltage

The effect of length to thickness concrete beam ratio

Figs. 12 and 13 Show that effect of length to thickness concrete column ratio on dynamic displacement according to blast. As it is observed, the concrete column dynamic displacement increases with increasing length to thickness

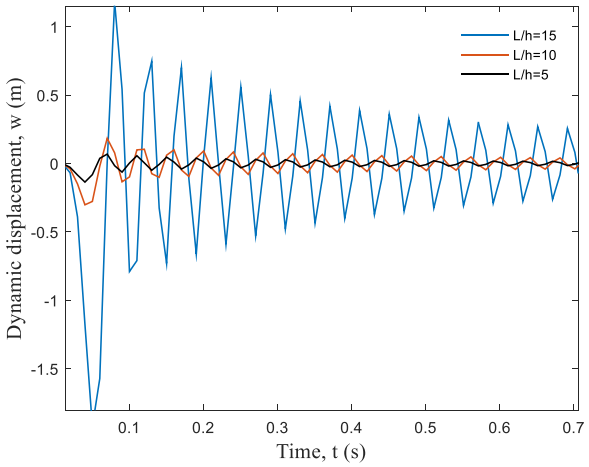

Fig. 13 The enlarged view of Fig. 12

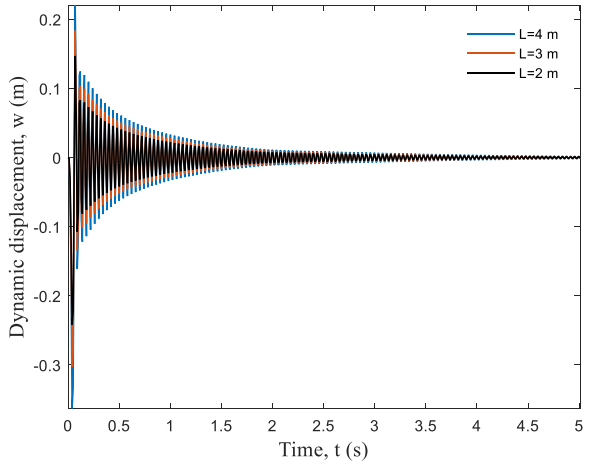

Fig. 14 Effect of concrete columns under the beam on the dynamic gradient of concrete beam with the application of external voltage

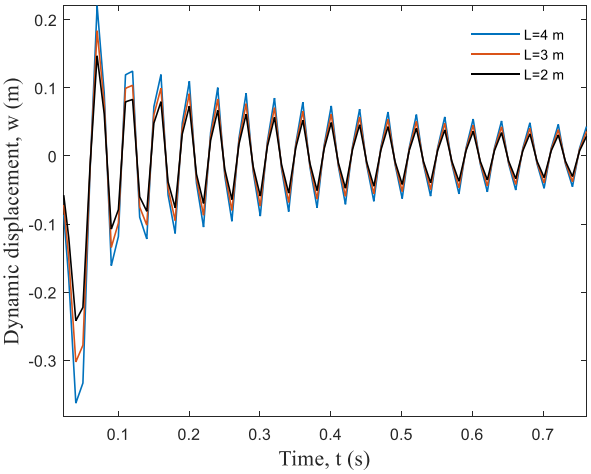

Fig. 15 The enlarged view of Fig. 14

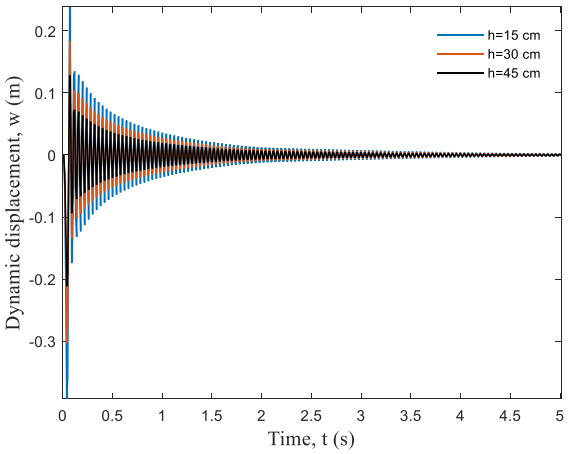

Fig. 16 The effect of concrete columns under the beam on the dynamic gradient of concrete beam without applying external voltage

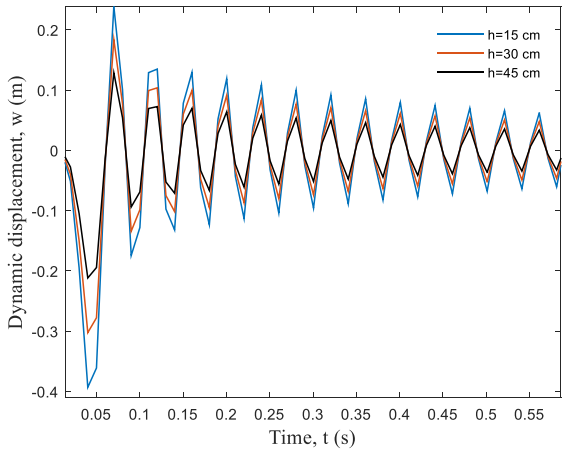

Fig. 17 The enlarged view of Fig. 16

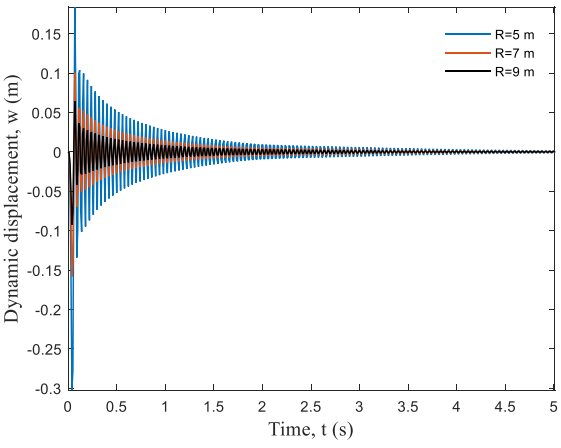

Fig. 18 The effect of the explosion distance to the concrete beam on the dynamic beam of concrete beam with the application of external voltage

concrete beam ratio, because it decreases structure stiffness. In other words, by increasing length to thickness concrete column ratio from 5 to 15, respectively, it becomes maximum dynamic displacement 0.1 and 0.15 meters, which shows an increase of 10 times dynamic displacement.

The effect of concrete beam length and thickness

Figs. 14 to 17, respectively, show the effect of concrete beams on structure dynamic displacement according to time. It can be observed that the dynamic displacement

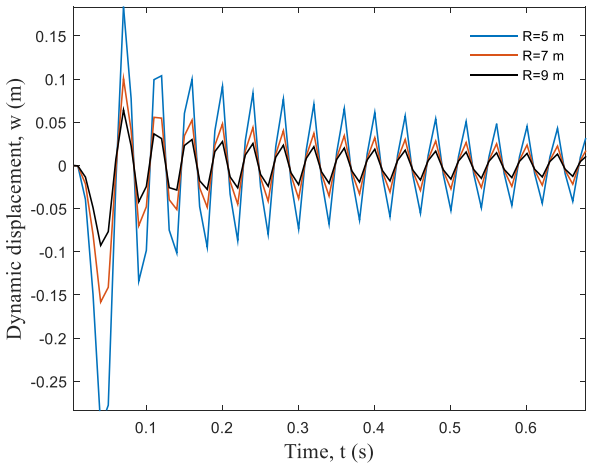

Fig. 19 The enlarged view of Fig. 18

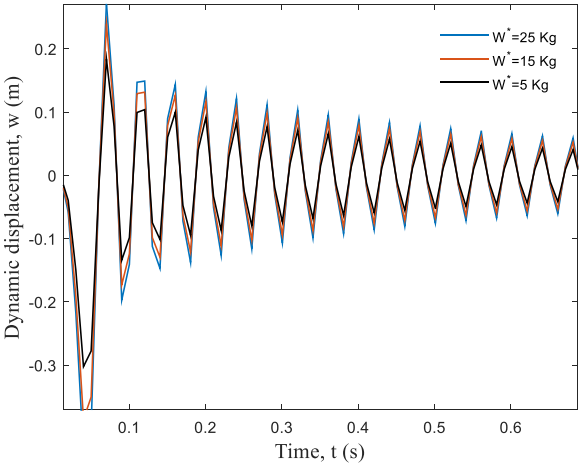

Fig. 21 The enlarged view of Fig. 20

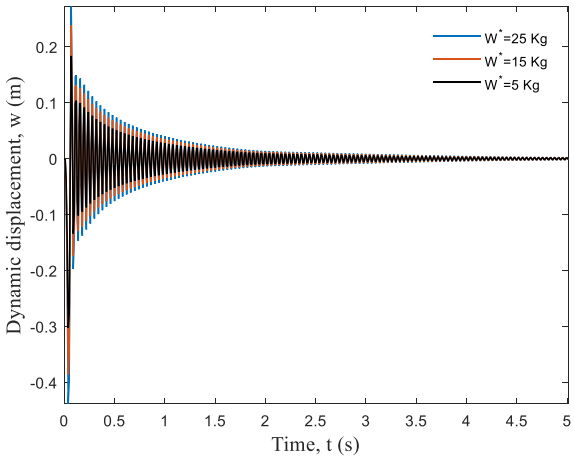

Fig. 20 The effect of the explosion distance to the concrete beam on the dynamic beam of concrete beam without the application of external voltage

increases by increasing length and reducing thickness of concrete beam, because it decreases structure stiffness.

The effect of blast load

Figs. 18 and 19 Show the impact of blast distance to concrete beam on dynamic displacement according to blast time. It is observed that concrete column dynamic displacement decreases by increasing blast distance to concrete beam, because the blast wave decreases.

Effect of blast amount is shown on dynamic displacement according to blast time in Figs. 20 and 21. As it can be observed the more increase in dynamic displacement of concrete beam, the more increase will be in the amount blast, due mainly to the increased rate in blast wave. Also, it decreases dynamic displacement by applying external voltage to structure.

14. Conclusions

In this study, the dynamic analysis of a concrete beam reinforced with silica nanoparticles subjected blast load was investigated. There's a concrete beam on two simply supports. For structural mathematical modeling, beam element and sinusoidal shear deformation theory are used. The governing equations on the structure were extracted using nonlinear strain-displacement, strain-strain, energy method and Hamilton principle. Finally, the dynamic displacement of the structure has been calculated using numerical methods of the square difference and Newmark. The effect of different parameters on the dynamic displacement of concrete beam was investigated such as effect volumetric and packing volumes of nanoparticles, geometric parameters of the beam, boundary conditions and blast load. The following results are obtained according to the drawn charts:

The larger the percentage of nanoparticles, the lower the dynamic gravity of the concrete beam is. The maximum dynamic gradient for states C_r=0 and C_r=2% states is respectively 0.23 and 0.19 meters, which indicates a decrease of about 20% dynamic gravity by increasing the volumetric percent of silica nanoparticles.

- Considering the accumulation, it caused a decrease in stiffness of structure and as a result, increased the dynamic displacement of concrete beam. For example, the maximum dynamic deflection of concrete beam for a state with and without nanoparticle accumulation is 0.15 and 0.055 m respectively, which indicates that the dynamic deflection of concrete beam is decreased by 67% for distribution condition of nanoparticles in concrete without accumulation.
- Concrete beam with curved and simple boundary conditions at the two ends is respectively with a maximum dynamic gradient of 0.9 and 0.18 meters. In other words, a concrete beam with boundary conditions leads to a decrease of about 50% of the maximum dynamic gradient relative to a concrete beam with simple boundary conditions.
- By increasing the ratio of length to thickness of the concrete column from 5 to 15, respectively, the dynamic gradient is maximum 0.1 and 1.05 meters. This indicates that the maximum dynamic gradient is increased 10 times.
- By increasing the length and reducing the thickness of

concrete beam, the dynamic displacement increases because stiffness of structure is decreased.

• By increasing the amount of blast, the dynamic displacement concrete beam increased becausethe wave increased due to blast.

• By increasing the blast distance to concrete beam, Reduced the dynamic displacement of concrete beam, becausethe wave was reduced due to blast**.**

References

Ahouel, M., Houari, M.S.A., Adda Bedia, E.A. and Tounsi, A. (2016), "Size-dependent mechanical behavior of functionally graded trigonometric shear deformable nanobeams including neutral surface position concept", *Steel Compos. Struct*., **20**(5), 963-981.

Alhatmey, I.A., Ekmekyapar, T. and Alrebeh, S.K. (2018), "Residual strength capacity of fire-exposed circular concrete-filled steel tube stub columns", *Adv. Concrete Concrete*, **6**, 485-507.

Arbabi, A., Kolahchi, R. and Rabani Bidgoli, M. (2017), "Concrete columns reinforced with Zinc Oxide nanoparticles subjected to electric field: buckling analysis", *Wind Struct*., **24**, 431-446.

Attia, A., Tounsi, A., Adda Bedia, E.A. and Mahmoud, S.R. (2015), "Free vibration analysis of functionally graded plates with temperature-dependent properties using various four variable refined plate theories", *Steel Compos. Struct*., **18**(1), 187-212.

Belabed, Z., Houari, M.S.A., Tounsi, A., Mahmoud, S.R. and Bég, O.A. (2014), "An efficient and simple higher order shear and normal deformation theory for functionally graded material (FGM) plates", *Compos.: Part B*, **60**, 274-283.

Beldjelili, Y., Tounsi, A. and Mahmoud, S.R. (2016), "Hygro-thermo-mechanical bending of S-FGM plates resting on variable elastic foundations using a four-variable trigonometric plate theory", *Smart Struct. Syst*., **18**(4), 755-786.

Belkorissat, I., Houari, M.S.A., Tounsi, A. and Hassan, S. (2015), "On vibration properties of functionally graded nano-plate using a new nonlocal refined four variable model", *Steel Compos. Struct*., **18**(4), 1063-1081.

Bellifa, H., Benrahou, K.H., Bousahla, A.A., Tounsi, A. and Mahmoud, S.R. (2017), "A nonlocal zeroth-order shear deformation theory for nonlinear postbuckling of nanobeams", *Struct. Eng. Mech*., **62**(6), 695-702.

Bellifa, H., Benrahou, K.H., Hadji, L., Houari, M.S.A. and Tounsi, A. (2016), "Bending and free vibration analysis of functionally graded plates using a simple shear deformation theory and the concept the neutral surface position", *J Braz. Soc. Mech. Sci. Eng*., **38**(1), 265-275.

Bennoun, M., Houari, M.S.A. and Tounsi, A. (2016), "A novel five variable refined plate theory for vibration analysis of functionally graded sandwich plates", *Mech. Adv. Mater. Struct*., **23**(4), 423-431.

Bessaim, A., Houari, M.S.A. and Tounsi, A. (2013), "A new higher-order shear and normal deformation theory for the static and free vibration analysis of sandwich plates with functionally graded isotropic face sheets", *J. Sandw. Struct. Mater*., **15**(6), 671-703.

Besseghier, A., Houari, M.S.A., Tounsi, A. and Hassan, S. (2017), "Free vibration analysis of embedded nanosize FG plates using a new nonlocal trigonometric shear deformation theory", *Smart Struct. Syst*., **19**(6), 601-614.

Bouafia, Kh., Kaci, A., Houari M.S.A. and Tounsi, A. (2017), "A nonlocal quasi-3D theory for bending and free flexural vibration behaviors of functionally graded nanobeams", *Smart Struct. Syst*., **19**, 115-126.

Bouderba, B., Houari, M.S.A. and Tounsi, A. (2013), "Thermomechanical bending response of FGM thick plates resting on Winkler-Pasternak elastic foundations", *Steel Compos. Struct*., **14**(1), 85-104.

Bouderba, B., Houari, M.S.A., Tounsi, A. and Mahmoud, S.R. (2016b), "Thermal stability of functionally graded sandwich plates using a simple shear deformation theory", *Struct. Eng. Mech*., **58**(3), 397-422.

Boukhari, A., Atmane, H.A., Tounsi, A., Adda Bedia, E.A. and Mahmoud, S.R. (2016), "An efficient shear deformation theory for wave propagation of functionally graded material plates", *Struct. Eng. Mech*., **57**(5), 837-859.

Bounouara, F., Benrahou, K.H., Belkorissat, I. and Tounsi, A. (2016), "A nonlocal zeroth-order shear deformation theory for free vibration of functionally graded nanoscale plates resting on elastic foundation", *Steel Compos. Struct*., **20**(2), 227-249.

Bourada, M., Kaci, A., Houari, M.S.A. and Tounsi, A. (2015), "A new simple shear and normal deformations theory for functionally graded beams", *Steel Compos. Struct*., **18**(2), 409-423.

Bousahla, A.A., Benyoucef, S., Tounsi, A. and Mahmoud, S.R. (2016a), "On thermal stability of plates with functionally graded coefficient of thermal expansion", *Struct. Eng. Mech*., **60**(2), 313-335.

Chikh, A., Tounsi, A., Hebali, H. and Mahmoud, S.R. (2017), "Thermal buckling analysis of cross-ply laminated plates using a simplified HSDT", *Smart Struct. Syst*., **19**(3), 289-297.

Draiche, K., Tounsi, A. and Mahmoud, S.R. (2016), "A refined theory with stretching effect for the flexure analysis of laminated composite plates", *Geomech. Eng*., **11**, 671-690.

Duc, N.D., Quan, T.Q. and Khoa, N.D. (2017), "New approach to investigate nonlinear dynamic response and vibration of imperfect functionally graded carbon nanotube reinforced composite double curved shallow shells subjected to blast load and temperature", *Aerosp. Sci. Tech*., **71**, 360-372.

Dutta, G., Panda. S.K., Mahapatra, T.R. and Singh, V.K. (2017), "Electro-magneto-elastic response of laminated composite plate: A finite element approach", *Int. J. Appl. Comput. Math*., **3**, 2573-2592.

El-Haina, F., Bakora, A., Bousahla, A.A. and Hassan, S. (2017), "A simple analytical approach for thermal buckling of thick functionally graded sandwich plates", *Struct. Eng. Mech*., **63**(5), 585-595.

Formica, G., Lacarbonara, W. and Alessi, R. (2010), "Vibrations of carbon nanotube reinforced composites", *J. Sound Vib*., **329**, 1875-1889.

Jafarian Arani, A. and Kolahchi, R. (2016), "Buckling analysis of embedded concrete columns armed with carbon nanotubes", *Comput. Concete*, **17**, 567-578.

Kadoli, R. and Ganesan, N. (2003), "Free vibration and buckling analysis of composite cylindrical shells conveying hot fluid", *Compos. Struct*., **60**, 19-32.

Khetir, H., Bouiadjra, M.B., Houari, M.S.A., Tounsi, A. and Mahmoud, S.R. (2017), "A new nonlocal trigonometric shear deformation theory for thermal buckling analysis of embedded nanosize FG plates", *Struct. Eng. Mech*., **64**(4), 391-402.

Kolahchi, R., RabaniBidgoli, M., Beygipoor, Gh. and Fakhar, M.H. (2013), "A nonlocal nonlinear analysis for buckling in embedded FG-SWCNT-reinforced microplates subjected to magnetic field", *J. Mech. Sci. Technol*., **5**, 2342-2355.

Kolahchi, R., Safari, M. and Esmailpour, M. (2016), "Dynamic stability analysis of temperature-dependent functionally graded CNT-reinforced visco-plates resting on orthotropic elastomeric medium", *Compos. Struct*., **150**, 255-265.

Larbi Chaht, F., Kaci, A., Houari, M.S.A. and Hassan, S. (2015),

"Bending and buckling analyses of functionally graded material (FGM) size-dependent nanoscale beams including the thickness stretching effect", *Steel Compos. Struct*., **18**(2), 425-442.

Lei, Z.X., Zhang, L.W., Liew, K.M. and Yu, J.L. (2014), "Dynamic stability analysis of carbon nanotubereinforced functionally graded cylindrical panels using the element-free kp-Ritz method", *Compos. Struct*., **113**, 328-338.

Liew, K.M., Lei, Z.X., Yu, J.L. and Zhang, L.W. (2014), "Postbuckling of carbon nanotube-reinforced functionally graded cylindrical panels under axial compression using a meshless approach", *Comput. Meth. Appl. Mech. Eng*., **268**, 1-17.

Mahapatra, T.R. and Panda, S.K. (2016a), "Nonlinear free vibration analysis of laminated composite spherical shell panel under elevated hygrothermal environment: A micromechanical approach", *Aerosp. Sci. Technol*., **49**, 276-288.

Mahapatra, T.R., Panda, S.K. and Kar, V.R. (2016b), "Nonlinear flexural analysis of laminated composite panel under hygro-thermo-mechanical loading-A micromechanical approach", *Int. J. Comput. Meth*., **13**, 1650015.

Mahapatra, T.R., Panda, S.K. and Kar, V.R. (2016c), "Nonlinear hygro-thermo-elastic vibration analysis of doubly curved composite shell panel using finite element micromechanical model", *Mech. Adv. Mater. Struct*., **23**, 1343-1359.

Mahapatra, T.R., Panda, S.K. and Kar, V.R. (2016d), "Geometrically nonlinear flexural analysis of hygro-thermo-elastic laminated composite doubly curved shell panel", *Int. J. Mech. Mat. Des*., **12**, 153-171.

Mahi, A., Bedia, E.A.A. and Tounsi, A. (2015), "A new hyperbolic shear deformation theory for bending and free vibration analysis of isotropic, functionally graded, sandwich and laminated composite plates", *Appl. Math. Model*., **39**, 2489-2508.

Matsuna, H. (2007), "Vibration and buckling of cross-ply laminated composite circular cylindrical shells according to a global higher-order theory", *Int. J. Mech. Sci*., **49**, 1060-1075.

Menasria, A., Bouhadra, A., Tounsi, A. and Hassan, S. (2017), "A new and simple HSDT for thermal stability analysis of FG sandwich plates", *Steel Compos. Struct*., **25**(2), 157-175.

Messina, A. and Soldatos, K.P. (1999), "Vibration of completely free composite plates and cylindrical shell panels by a higher-order theory", *Int. J. Mech. Sci*., **41**, 891-918.

Metsebo J., Nana Nbendjo, B.R. and Woafo, P. (2016), "Dynamic responses of a hinged-hinged Timoshenko beam with or without a damage subject to blast loading", *Mech. Res. Commun.*, **71**, 38-43.

Meziane, M.A.A., Abdelaziz, H.H. and Tounsi, A.T. (2014), "An efficient and simple refined theory for buckling and free vibration of exponentially graded sandwich plates under various boundary conditions", *J. Sandw. Struct. Mater*., **16**(3), 293-318.

Mori, T. and Tanaka, K. (1973), "Average stress in matrix and average elastic energy of materials with misfitting inclusions", *Acta Metall. Mater*., **21**, 571-574.

Motezaker, M. and Kolahchi, R. (2017), "Seismic response of SiO2 nanoparticles-reinforced concrete pipes based on DQ and newmark methods", *Comput. Concrete*, **19**(6), 751-759.

Mouffoki, A., Adda Bedia, E.A., Houari, M.S.A. and Hassan, S. (2017), "Vibration analysis of nonlocal advanced nanobeams in hygro-thermal environment using a new two-unknown trigonometric shear deformation beam theory", *Smart Struct. Syst*., **20**(3), 369-383.

Seo, Y.S., Jeong, W.B., Yoo, W.S. and Jeong, H.K. (2015), "Frequency response analysis of cylindrical shells conveying fluid using finite element method", *J. Mech. Sci. Tech*., **19**, 625-633.

Shi, D.L. and Feng, X.Q. (2004), "The effect of nanotube waviness and agglomeration on the elastic property of carbon nanotube-reinforced composties", *J. Eng. Mater. Tech*., ASME, **26**, 250-270.

Shim, C.S., Lee, C.D. and Ji, S.W. (2018), "Crack control of precast deck loop joint using high strength oncrete", *Adv. Concrete Concrete*, **6**, 527-543.

Solhjoo, S. and Vakis, A.I. (2015), "Single asperity nanocontacts: Comparison between molecular dynamics simulations and continuum mechanics models", *Comput. Mater. Sci*., **99**, 209-220.

Suman, S.D., Hirwani, C.K., Chaturvedi, A. and Panda, S.K. (2017), "Effect of magnetostrictive material layer on the stress and deformation behaviour of laminated structure", *IOP Conference Series: Materials Science and Engineering*, **178**(1), 012026.

Tan, P. and Tong, L. (2001), "Micro-electromechanics models for piezoelectric-fiber-reinforced composite materials", *Compos. Sci. Tech*., **61**, 759-769.

Thai, H.T. and Vo, T.P. (2012), "A nonlocal sinusoidal shear deformation beam theory with application to bending, buckling, and vibration of nanobeams", *Int. J. Eng. Sci*., **54**, 58-66.

Wuite, J. and Adali, S. (2005), "Deflection and stress behaviour of nanocomposite reinforced beams using a multiscale analysis", *Compos. Struct*., **71**, 388-396.

Zamanian, M., Kolahchi, R. and Rabani Bidgoli, M. (2017), "Agglomeration effects on the buckling behaviour of embedded concrete columns reinforced with SiO2 nano-particles", *Wind Struct.*, **24**, 43-57.

Zemri, A., Houari, M.S.A., Bousahla, A.A. and Tounsi, A. (2015), "A mechanical response of functionally graded nanoscale beam: an assessment of a refined nonlocal shear deformation theory beam theory", *Struct. Eng. Mech*., **54**(4), 693-710.

Zidi, M., Tounsi, A. and Bég, O.A. (2014), "Bending analysis of FGM plates under hygro-thermo-mechanical loading using a four variable refined plate theory", *Aerosp. Sci. Tech*., **34**, 24-34.

CC